



Host B cells escape CAR-T immunotherapy by reversible downregulation of CD19

Sara Fioretti¹ · Courtney A. Matson¹ · Kenneth M. Rosenberg¹ · Nevil J. Singh¹

Received: 9 November 2021 / Accepted: 24 May 2022 / Published online: 26 June 2022
© The Author(s), under exclusive licence to Springer-Verlag GmbH Germany, part of Springer Nature 2022

Abstract

Anti-CD19-CAR-T cells are a successful clinical immunotherapy for B cell lymphomas, although some lymphomas can escape attack by downregulating surface CD19 levels. An undesirable consequence of this therapy is that it can also eliminate healthy B cells expressing CD19. Therefore, understanding the dynamics of CD19 expression in B cells under CAR-T cell immunotherapy can help mitigate both escape and adverse outcomes. Previous studies suggested that mechanisms responsible for the loss of CD19 expression in lymphomas usually involves genomic deletion or epigenetic modification which permanently removes CD19 as a therapeutic target in these cells. We examined if healthy B cells can use similar processes to lose CD19 expression and escape CAR-T attack. In the presence of CAR-T cells, untransformed B cells both when cultured in vitro or in vivo in non-tumor bearing animals downregulate expression of CD19. We then used adoptive transfer strategies to remove CD19-low B cells from α CD19-CAR-T pressure in vivo. Intriguingly, these B cells systematically recovered surface expression of CD19 comparable to wild-type levels. These data suggest that unlike many cases of lymphomas, healthy B cells downregulate CD19 in a reversible fashion. Taken together, these data suggest a dynamic regulatory process of CD19 surface expression on healthy B cells that could be exploited to modulate the expression of CD19 on cancer cells to improve immunotherapy or minimize the depletion of endogenous B cell compartment during treatment.

Keywords CAR-T · B cell · CD19 · Immunotherapy

Introduction

Chimeric antigen receptor T cell (CAR-T cell) therapy has transformed the field of immunotherapy by combining specific native antigen recognition of antibodies with the cytotoxic potential of the T cell receptor signaling machinery. This produces an effective mechanism for eliminating cancer cells as evidenced by its success in the clinic, particularly with B cell lymphomas [1]. B cell lymphomas are ideal CAR-T targets since they have antigens restricted to tumors and healthy B cell populations such as CD19 [2–4]. CD19-CAR-T cells have 70% or greater complete remission in patients with acute lymphoblastic leukemia (ALL) which

demonstrates their efficacy and therapeutic use [5]. Additional CAR-T targets such as CD20, CD22, and BCMA are being tested but approval and usage of CD19 was the first successful CAR-T therapy.

Despite success in many patients, there are significant adverse events including, but not limited to: cytokine release syndrome, neurotoxicity, cardiovascular toxicity, and metabolic complications [6]. Additionally, cases of relapse are present in more than half of treated patients [5]. Relapses include both CD19+ and CD19- populations of cells, where CD19+ relapses likely result from defects in CD19-CAR-T therapy itself such as death and exhaustion, whereas CD19- relapses arise from intrinsic alterations within the tumor [7]. The rising incidence of relapse, particularly CD19- relapses, provides a significant therapeutic hurdle that warrants a deeper investigation into alternative targets or better execution of CD19-CAR-T therapies.

It is currently thought that CD19- relapses arise through genomic mutations or through an epigenetic switch of cell lineage. Samples from relapsed CD19- patients have hemizygous deletions of the *CD19* locus, de novo frameshift and

S. Fioretti and C.A. Matson contributed equally to this work.

✉ Nevil J. Singh
nsingh@som.umaryland.edu

¹ Department of Microbiology and Immunology, University of Maryland School of Medicine, 685 West Baltimore Street HSF1, Room 380, Baltimore, MD 21201, USA

missense mutations, and alternatively spliced *CD19* mRNA resulting in the loss of CD19-CAR-T targeting [8]. The first two of these mutations occur at the level of the genome and result in the permanent loss of CD19, eliminating the use of CD19-CAR-T therapies. In contrast, the alternative splice variant may provide a temporal level of control on the expression of CD19 in the tumor cells, but this has yet to be explored further. Moreover, a recent study described epigenetic silencing of CD19 expression in a humanized mouse model of chronic lymphocytic leukemia (CLL) that is reversible upon administration of demethylating agents [9]. In addition to these mechanisms, CD19-CAR-T therapy can induce a lineage switch in B-ALL through downregulation of B cell master transcription factors like *Pax5* [10]. This results in the loss of the B cell phenotype and concurrent acquisition of myeloid markers. This occurs through chromatin remodeling to express myeloid markers after CD19-CAR-T treatment and remained stable after the removal from CD19-CAR-T pressure [10]. This demonstrates the wide variety of methods, many of which result in permanent loss of CD19 expression, that tumor cells use to adapt and prevent targeting from CD19-CAR-T therapy.

As mentioned above, healthy B cells also express CD19 and are also subjected to CD19-CAR-T-mediated killing during therapy [11]. Patients are left with B cell aplasia while maintaining some plasma cells. With the current concern of tumor escape and development of additional CAR-T targets, other populations of B cells such as plasma cells will become ‘on-target, off-tumor’ bystanders of BCMA-CAR-T therapies resulting in significant impacts on humoral immunity after treatment highlighting the need for optimizing immunotherapies. Interestingly, there are instances of healthy B cells escaping CD19-CAR-T mediated killing but the mechanisms by which this happens are ill defined [12, 13]. As such, it is imperative to understand the existing mechanisms that healthy B cells utilize to escape CAR-T mediated killing and how they could be hijacked by cancer cells for escape. Another significant value in understanding the mechanisms of healthy B cell killing and target escape is that CAR-T cells which trogocytose CD19 are also subject to fratricide [14]. The role of host CD19 in facilitating such a killing of CAR-T cells themselves is not well-understood. However, reducing healthy B cell killing can also augment tumor immunotherapy in this context.

In this report, we find that healthy B cells transiently downregulate CD19 upon exposure to CD19-CAR-T cells. Upon re-transfer into CAR-T free hosts, the CD19-downregulated B cells recover CD19 expression comparable to wild-type levels demonstrating the dynamic regulation of this molecule as a homeostatic cellular phenomenon. This suggests that unlike most previously described mechanisms of tumor escape through permanent downregulation of CD19, healthy B cells transiently alter CD19 expression

depending upon environmental pressures. By further studying the molecular mechanisms that underlie this process, strategies could be developed to improve immunotherapies to subvert tumor escape and eliminate the need for secondary CAR-T targets.

Results

CD19-CAR-T cells are activated in response to healthy splenocyte co-culture in vitro

The mechanisms of CD19 downregulation and immunotherapy escape by lymphoma cells has been well-studied using mouse models [8, 9, 13, 15, 16]. We used a similar strategy here to examine how normal B cells in a healthy animal can escape CAR-T cells. CD19-CAR-T cells were generated using a retroviral expression system, as previously described [11]. Briefly, the CD19-CAR-T constructs containing the scFV region from 1D3 was packaged to prepare retroviral stocks. Primary T cells were isolated and purified from wild-type mice and activated using anti-CD3 and anti-CD28. The T cells were transduced and expression of the CD19-CAR-T receptor was measured by flow cytometric analysis (Fig. 1A). To determine whether the cells expressing the CD19-CAR-T receptor were functionally active, we co-cultured CD19-CAR-T cells with varied numbers of healthy splenocytes from T cell deficient animals to eliminate endogenous T cell responses. After 24 and 48 h of culture, we analyzed the expression of the activation markers CD69 and CD25 on CD19-CAR-T cells. At 24 h after activation, most of the T cells in the culture increased CD69 expression (Fig. 1B). At 48 h, there was an increase in the frequency of CD25 + T cells (Fig. 1C, left panels) and expression levels of CD25 (Fig. 1C, right panels). Taken together, these data validate that CD19-CAR-T cells are activated when exposed to healthy splenocytes similar to previous findings [12].

Healthy B cells downregulate CD19 after CAR-T exposure in vitro

To determine whether the activated CD19-CAR-T cells alter B cells, we co-cultured CAR-T cells and monitored the frequency of CD19 B cells in culture over 48 h. Staining for B220 together with CD19 at the same time allowed us to discriminate killing of healthy B cells from modulation of CD19 levels. B cells were identified as live, TCR β -, and B220 + (Fig. 2A). In these cultures, the target population of CD19 + B220 + frequency ranged from 52.0 to 66.6% of splenocytes across all experiments for a total of $5.2\text{--}6.6 \times 10^5$ target cells per culture. After 48 h, there was a loss in frequency of CD19 + B cells at the highest concentration of CD19-CAR-T cells (Fig. 2B and C, top panel).

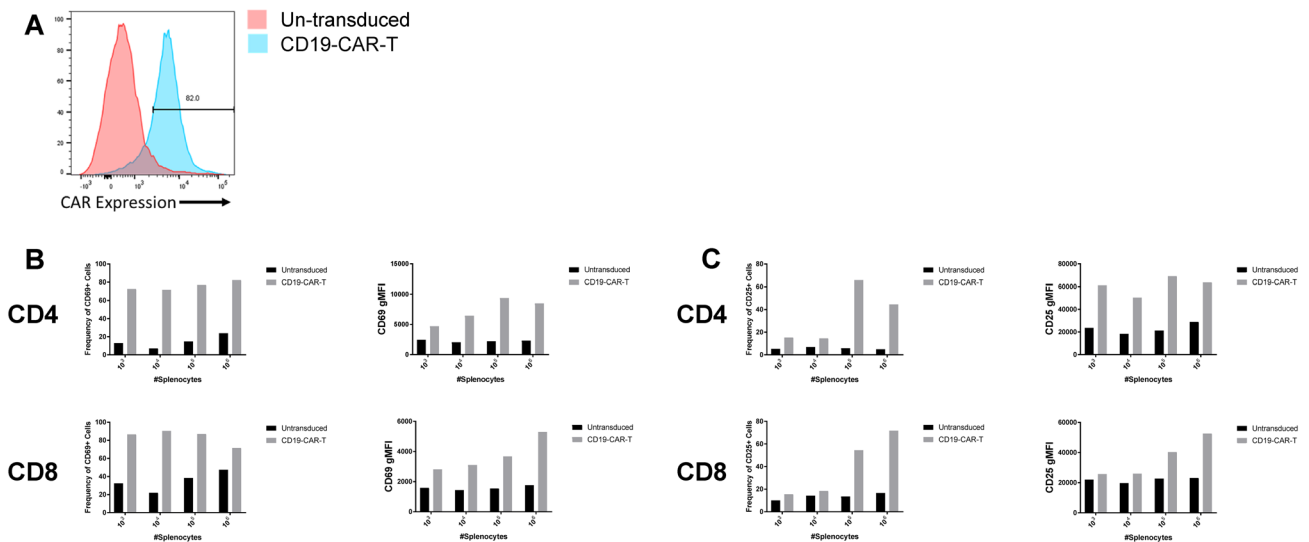


Fig. 1 Generation of functional CD19-CAR-T cells. **A** Wild-type splenocytes were harvested, purified, and activated for 48 h. Activated cells were retrovirally transduced to express CD19-CAR receptor. 48 h after second transduction, cells were harvested and analyzed for CD19-CAR-T receptor expression via flow cytometric analysis. Representative histogram showing CD19-CAR expression. **B** 2×10^5 CD19-CAR-T cells were co-cultured with healthy splenocytes at indicated densities from T cell deficient animals. Co-cultures were

harvested at 24 h to assess CD69 frequency (left panel) and gMFI (right panel) of CD4 (top) and CD8 (bottom) T cells ($n=1$ from 1 independent experiment). **C** 2×10^5 CD19-CAR-T cells were co-cultured with healthy splenocytes at indicated densities from T cell deficient animals. Co-cultures were harvested at 48 h to assess CD25 frequency (left panel) and gMFI (right panel) of CD4 (top) and CD8 (bottom) T cells ($n=1$ from 1 independent experiment)

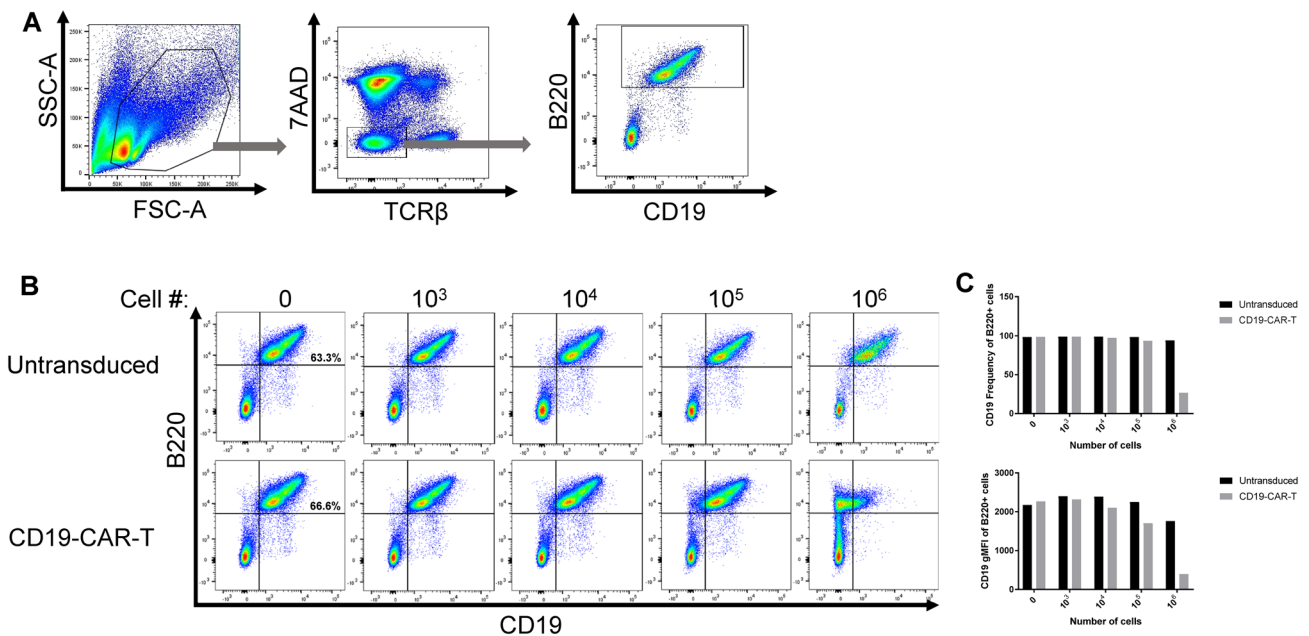


Fig. 2 Co-culture of CD19-CAR-T cells with healthy splenocytes induces downregulation of CD19 on B cells. **A** Gating strategy for analyzing CD19 expression on B220+B cells from co-culture of splenocytes from T-cell deficient animals and CD19-CAR-T or untransduced cells. **B** Representative flow plots from CD19-CAR-T or untransduced cells at indicated densities were co-cultured with

1×10^6 healthy splenocytes ($n=2$ from 2 independent experiments). CD19+B220+target cell frequency ranged from 52.0–66.6% of splenocytes across all experiments for a target population range of $5.2\text{--}6.6 \times 10^5$ cells per culture. **C** CD19 frequency (top panel) and gMFI (bottom panel) on live B220+B cells from co-culture ($n=2$ from 2 independent experiments, representative values shown)

Interestingly, there was a decrease in CD19 gMFI on the remaining live B220+ cells as well (Fig. 2B and C, bottom panel). These data suggest that in vitro healthy B cells downregulate CD19 when exposed to CD19-CAR-T cells similar to previous findings [12].

In vivo transfer of CD19 CAR-T cells to non-tumor bearing animals results in CD19 downregulation on healthy B cells

To evaluate whether the downregulation of CD19 on healthy B cells was an in vitro phenomenon of co-culture with CD19-CAR-T cells, we transferred CD19-CAR-T cells or untransduced cells into healthy T-cell deficient animals and monitored the expression of CD19 on B cells. After 10 days, splenocytes and lymph nodes were harvested to evaluate CD19 expression (Figure 3A). CD19 expression is downregulated in CD19-CAR-T animals, although it does not reach statistical significance (Figure 3C) due to biological variation in the CD19-CAR-T treated animals as seen by the varied expression of CD19 on remaining B cells in the representative flow plots in Figure 3B. Prior to the day 10 endpoint, animals were bled to monitor the frequency of CD19+ B cells (Figure 3D, top panel) and CD19 expression

(Figure 3D, bottom panel). There was no significant loss of CD19+ cell frequency when compared to untransduced cells through day 7 (Figure 3D). Interestingly, one animal did have a loss of CD19 frequency compared to the others in the CD19-CAR-T treated cohort by day 7 after transfer indicating that there is loss of CD19 by this timepoint but there is large biological variation within the system (Figure 3D, top panel). Taken together these data suggest that there is active downregulation of CD19 on B cells exposed to CD19-CAR-T therapy in vivo supporting previous findings [12, 13].

CD19 expression is recovered in vivo after removal from CAR-T exposure

Considering that the downregulation of CD19 provides an escape mechanism for healthy B cells from being targeted by CAR-T therapy, we wanted to understand the dynamics of CD19 expression on healthy B cells that had undergone downregulation after CD19-CAR-T exposure. Similar to the experiments described in Figure 3, we transferred CD19-CAR-T or untransduced cells into healthy T-cell deficient animals to induce CD19 downregulation on B cells. We then harvested lymph nodes and splenocytes from these animals and sorted B cells from CD19-CAR-T exposed animals and

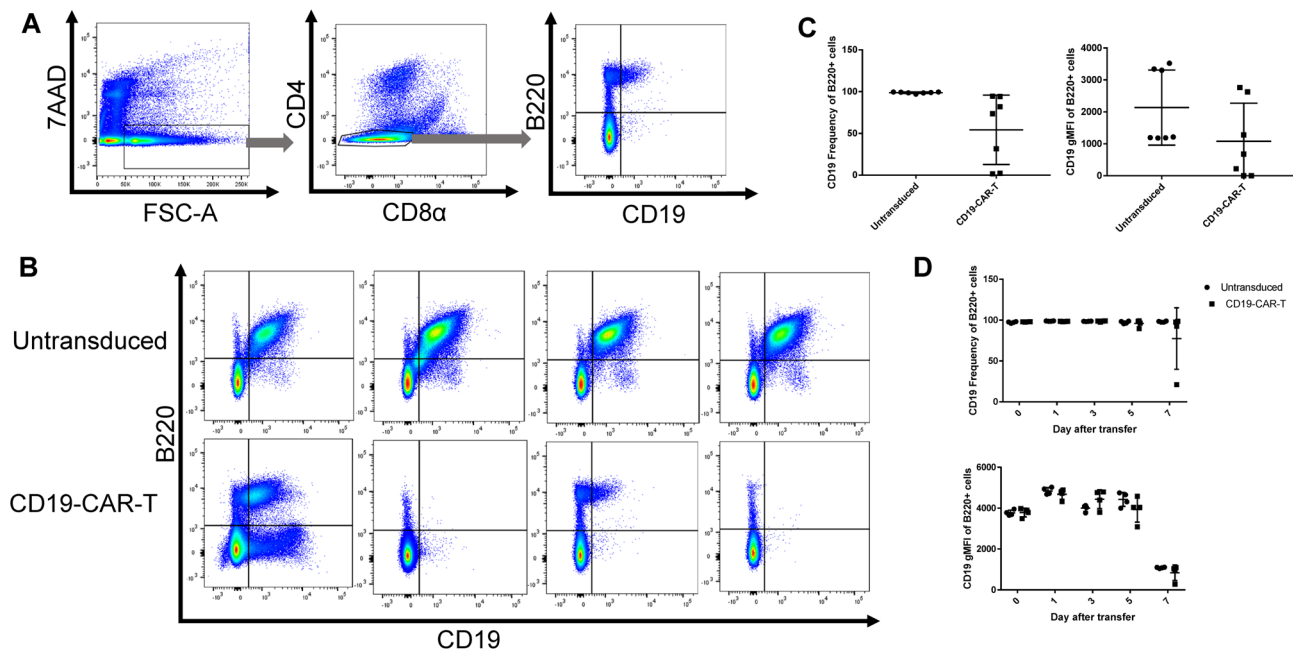


Fig. 3 Adoptive transfer of CD19-CAR-T cells induces dynamic downregulation of CD19 on healthy B cells in the absence of a tumor. **A** Gating strategy for analyzing CD19 expression on B220+ B cells in a pooled sample containing both lymph nodes and spleen from T-cell deficient animals 10 days after adoptive transfer of 4×10^6 CD19-CAR-T or untransduced cells. Plots displayed are derived from a representative CAR-T treated animal. **B** Representative flow plots of B220+ B cells from animals 10 days after adoptive transfer of CD19-

CAR-T or untransduced cells as described in (A) ($n=7$ from 2 independent experiments). **C** CD19 frequency (left panel) and gMFI (right panel) of B220+ B cells from animals 10 days after adoptive transfer of CD19-CAR-T or untransduced cells as described in (A) ($n=7$ from 2 independent experiments). **D** CD19 frequency (top panel) and gMFI (bottom panel) of B220+ B cells from animals prior to transfer or 1, 3, 5, or 7 days after adoptive transfer of CD19-CAR-T or untransduced cells ($n=4$ from 1 independent experiment)

adoptively transferred them into healthy, congenically distinct wild-type (T-cell sufficient) hosts without any CD19-CAR-T cells where they resided for 60 days (Figure 4A). Given the biological variability in CD19 downregulation on B cells in CD19-CAR-T exposed animals (Figure 3B, bottom panels), CD19-low and CD19-intermediate B cells were sorted and transferred into wild-type hosts (Figure 4B). After 60 days, the CD19-low and CD19-intermediate cells regained CD19 expression comparable to the endogenous B cells of the host (Figure 4C). Additionally, the frequency of CD19+ B cells and the expression of CD19 on B cells was not significantly different between the endogenous compartment and the CD19-low or CD19-intermediate transferred cells (Figure 4D). Taken together, these data demonstrate that the expression of CD19 is dynamic on healthy B cells in vivo. The pressure from CD19-CAR-T therapy can

downregulate surface expression but, upon removal from this context, B cells recover CD19 expression comparable to healthy levels.

Discussion

Here, we describe a mechanism by which healthy B cells dynamically regulate surface CD19 expression after CD19-CAR-T treatment in non-tumor bearing animals. Upon removal from CAR-T pressure, healthy B cells recover CD19 expression comparable to wild-type levels. This phenomena of CD19 downregulation likely provides a mechanism for preserving healthy B cells from CD19-CAR-T mediated killing. This would result in a reserve of B cells that could maintain humoral immunity, beyond

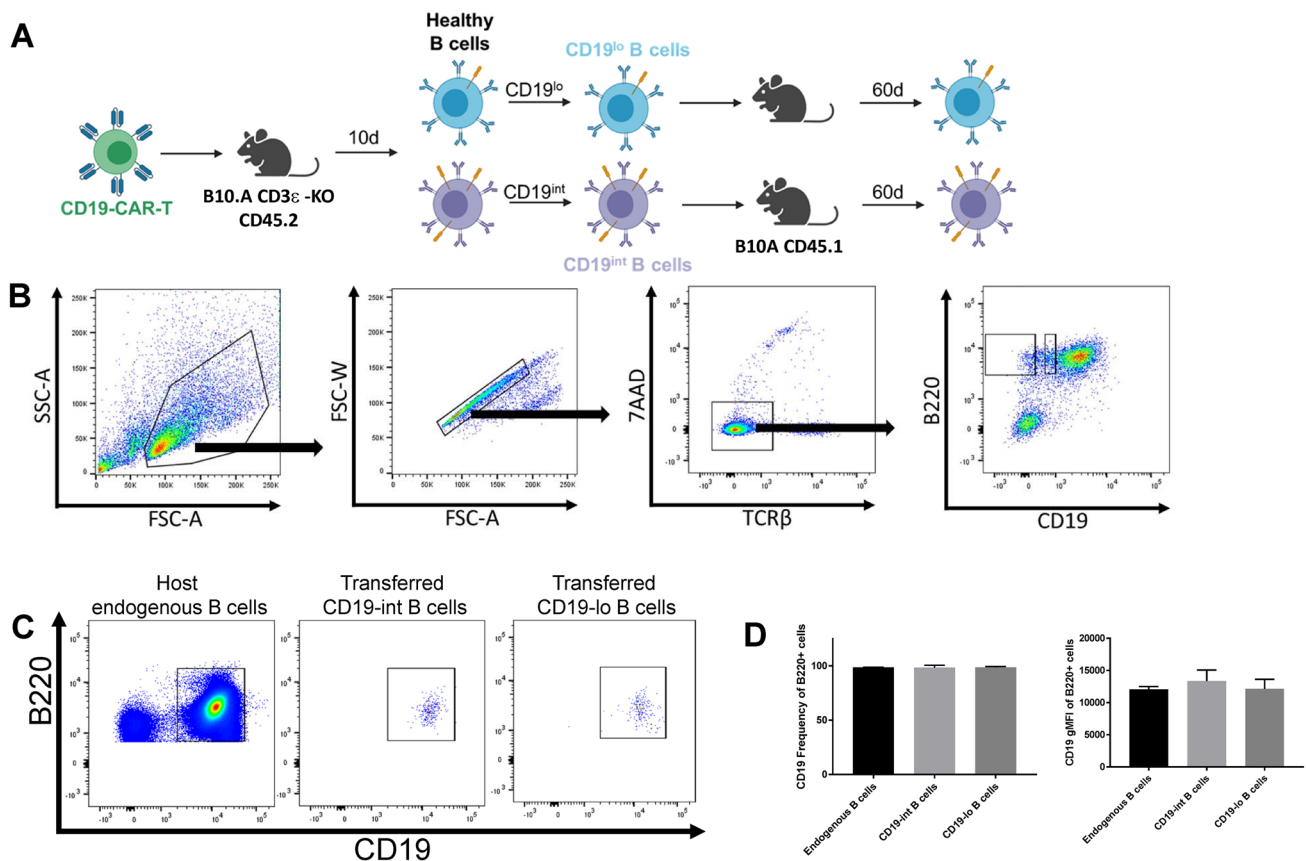


Fig. 4 Removal CD19-CAR-T pressure restores endogenous expression of CD19 on transferred CD19-downregulated B cells **A** Experimental outline. Images generated with BioRender.com. **B** Gating strategy for sorting CD19-lo and CD19-int B220+B cells isolated from lymph nodes and spleens from T-cell deficient animals 10 days after adoptive transfer of 4×10^6 CD19-CAR-T cells. Sample pooled from 3 CD19-CAR-T treated animals. **C** Sorted 2.2×10^5 CD19-lo or CD19-int B cells were adoptively transferred into congenically distinct wild-type hosts. Lymph nodes and spleens from adoptively transferred animals were harvested 60 days after transfer for flow

cytometric analysis. Representative plots of endogenous B cell populations, transferred CD19-int B cells, and transferred CD19-lo B cells isolated from pooled lymph node and spleen are shown ($n=3$ per transfer group, $n=6$ for endogenous populations, from 1 independent experiment). **D** CD19 frequency (left panel) and gMFI (right panel) of B220+B cells isolated from pooled lymph node and spleen from animals adoptively transferred with sorted CD19 B cell populations ($n=3$ per transfer group, $n=6$ for endogenous populations, from 1 independent experiment). Statistical analysis was performed using one-way ANOVA

plasma cells, and potentially recover expression of CD19 after CD19-CAR-T treatment. Moreover, it provides insight into the potential mechanisms that tumor cells may utilize to downregulate CD19 expression to escape CD19-CAR-T mediated killing.

The mechanisms of lymphoma escape from immunotherapy has been previously described [8, 9, 11, 13, 15–18]. These typically fall under two mechanisms—a transcriptional downregulation involving epigenetic changes or a lineage switch involving alterations in master regulators. Given that healthy B cells are capable of dynamic regulation of CD19 expression, this suggests that downregulation may be a homeostatic process. Healthy B cells undergo differentiation into plasma cells where there is a loss of typical B cell markers such as CD19. This transition is mediated by the loss of the *Pax5* transcription factor and the subsequent upregulation of *Blimp-1* which mediates the transcriptional program for long-lived plasma cell (LLPC) differentiation by inhibition of both *Pax5* and *Bcl-6* [17, 18]. This process is thought to be a permanent lineage switch due to this regulatory loop between *Blimp-1* and *Pax5*. Given these homeostatic mechanisms, it is not difficult to speculate that the cancer cells also likely possess similar mechanisms for CD19 downregulation which would eliminate the effective targeting via CD19-CAR-T. For example, recent studies have identified epigenetic modifications of the CD19 promoter that result in downregulation of CD19 expression that is reversible through pharmacological intervention [9]. Indeed, a similar mechanism could be occurring in healthy B cells as well. Understanding the different mechanisms could provide a novel therapeutic target to subvert escape mechanisms of relapsed cells by preventing the initial downregulation of CD19 or potentially restoring CD19 expression on CD19-malignant B cells. Given the widespread usage of anti-CD19 immunotherapy, the impact of these CAR-T cells on healthy B cells as well as the ability of the latter to escape killing by transient downregulation is of particular interest. If the mechanisms facilitating CD19 downregulation in lymphomas versus healthy cells are different, the latter could be targeted to spare them from CAR-T attack even before therapy. In this context, a recent study from Ledererova et al. [9] is illuminative. In this case, hypermethylation of the CD19 promoter allowed multiple CLLs to escape CAR-T attack. This downregulation was also recoverable unlike previously reported molecular genetic alterations or lineage switch; yet it remains to be seen whether this is a distinct mechanism or a downregulation of expression of the methyltransferases responsible. Indeed, these pathways could be druggable targets. In addition to keeping healthy B cells intact, such ‘CD19-downregulation’ pre-treatments could also help focus CAR-T cells better to the tumors. As mentioned in the introduction, this could come about also by a reduction in CAR-T fratricide.

Since there are other therapeutic CAR targets (CD20, BCMA, etc.) in development, exploring mechanisms of downregulation of their target molecules as well as the ‘on-target, off-tumor’ effects of those therapies may provide a better first therapeutic option given the escape phenotype seen with CD19-CAR-T treatment. Yet, there may be additional interactions between these surface molecules that have not yet been appreciated. For example, treatment with Rituximab, a CD20 monoclonal antibody treatment, induces CD19 downregulation without cell death through CD19 transfer to monocytes and neutrophils [19]. The authors suggest that this is likely through a Fc receptor-dependent, complement-independent mechanism due to the binding of Rituximab to CD20. This suggests that despite targeting CD20, there is still mechanisms that downregulate CD19. Additionally, this creates novel on-target, off-tumor populations of CD19+ monocytes and neutrophils that may be killed by CD19-CAR-T therapy if used subsequently. Taken together, this presents a larger potential issue where there is modulation of surface molecule expression that is not the CAR target itself and warrants exploration of the CD19 levels on patients treated with CD20-CAR-T therapies.

Materials and Methods

Cell Culture

Phoenix-GP cells were obtained from ATCC (ATCC® CRL-3215™) and maintained in DMEM (Gibco) supplemented with 10% FCS (Gemini), 2% glutamine (Gibco), 1% sodium pyruvate (Gibco), and 1% antibiotic/antimycotic (Gibco). Primary murine T cells were maintained in RPMI-1640 (Gibco) supplemented with 10% FCS (Gemini), 1% glutamine (Gibco), 1% antibiotic-antimycotic (Gibco), and 0.000014% β -mercaptoethanol (T cell media, TCM).

CD19-CAR Retrovirus Production

CD19-CAR retroviral constructs were obtained from Addgene (CAT# 107,226). This previously published construct used the scFV of the anti-mouse-CD19 clone 1D3, and the intracellular signaling domains of mouse CD28 and CD3 ζ ITAMs [11]. This construct was used to transfect Phoenix-GP cells (ATCC). Phoenix-GP cells were plated at a density of 4.5×10^6 cells per 10 cm plate and incubated overnight at 37C. Media was exchanged and cells were incubated for 1 h at 37C. Cells were transfected with lipofectamine in OptiMEM (Gibco) with 20 μ g of CD19-CAR retroviral plasmid and 10 μ g of pCL-ECO (Addgene CAT# 12,371). Cells were incubated for 10 h before media was exchanged. Retroviral supernatants were collected every 12 h for 72 h and spun for clarification and

removal of cell debris. Clarified supernatants were concentrated using three-part viral supernatant with one-part Retro-X (Takara CAT# 631,456). Solution was mixed through inversion and stored overnight at 4°C. Solution was centrifuged at 1500 g for 45 min at 4°C. Supernatant was removed, and viral pellet was resuspended in DMEM to be used for transduction.

Mice

Wild-type (WT) mice were obtained from both Jackson Laboratories (C57BL/6 J and B6.SJL-PtprcaPepcb/BoyJ) and Taconic Biosciences (B6NTac and B6.SJL-Ptprca/BoyAiTac). B6 mice were bred for dual congenic expression using a dam or sire from opposing place of purchase to eliminate any strain drift between the two WT strains. Wild-type B10.Q/Ai mice were originally obtained from Ron Schwartz, Institute of Allergy and Infection Diseases, NIH, Bethesda, MD. Wild-type B10.A-H2a H2-T18a/SgSnJ mice were obtained from Jackson laboratories. B10.A mice were bred for dual-congenic expression using a dam or sire from opposing genotypes. TCR- $\alpha\beta$ KO mice were obtained from the Jackson Laboratories (B6.129S2-Tcratm1Mom/J). CD3e knockout mice were obtained from NIAID/Taconic mouse contract (B10.A-Cd45a(Ly5a)/NAi N5). Animals were bred and maintained in modified specific pathogen-free facilities at the University of Maryland Baltimore Experiments were performed with animals at least 6 weeks of age and approved by University of Maryland Baltimore Institutional Animal Care and Use Committee.

Lymphocyte Isolation and Magnetic Depletion

Lymph node and spleen were isolated from mice and mechanically processed into single-cell suspensions by mashing tissues through a 100 μ M nylon mesh. The cell suspensions were then processed through a Ficoll-HiPaque Density Gradient to isolate lymphocytes. Magnetic depletion was performed with MyOne Streptavidin T1 DynaBeads with biotinylated anti-CD45R/B220 (RA3-6B2, Biolegend #103,204), biotinylated anti-NK1.1 (PK136, Biolegend #108,704), biotinylated anti-I-A/I-E (M5/114, Biolegend #107,604), and biotinylated anti-CD11b (M1/70, Biolegend #101,204) for isolation of CD4 and CD8 T cells according to the manufacturer's instructions.

Retroviral Transduction

Purified mouse T cell populations isolated from magnetic depletion were plated in TCM and stimulated with plate bound anti-CD3 ϵ (145-2C11, Biolegend CAT#100,302) and soluble anti-CD28 (37.51, Biolegend CAT#102,102)

to activate cells. After 30 h, T cells were transduced with CD19-CAR retrovirus or incubated without retrovirus using polybrene at an MOI of 1:10. Cells were spun at 2000 rpm for 2 h at 32°C to increase transduction efficiency. Cells were returned to 37°C incubator for 8 h. A second round of transduction was performed as described above to increase transduction efficiency of cells. Cells were rested for 48 h before harvest for flow cytometry analysis. CD19-CAR-T cells were maintained in TCM with supplementation of IL-2 at 10 IU/mL (Biolegend CAT# 714,604).

Flow Cytometry Staining

Fc-receptor blocking was performed for 15 min at 4 °C in 1 \times PBS supplemented with 2% FCS, 0.01% azide, 1% mouse serum, 1% hamster serum, and 1% rat serum (FcBlock). Surface staining was performed for 30 min at 4 °C in PBS supplemented with 2% FCS, 0.01% azide, and 0.02% EDTA (FACS Buffer) using the antibodies provided in Table 1. Cells were washed once with FACS Buffer. Stained cells were washed twice with FACS buffer. Cells were analyzed on an LSR-Fortessa flow cytometer (BD). All data were analyzed using FlowJo (Tree Star).

CD19-CAR-T and Splenocyte In Vitro Co-Culture Assay

CD19-CAR-T cells were combined with splenocytes in ratios as indicated in each experiment and co-cultured for 24–48 h in TCM. Cells were harvested from culture conditions for flow cytometric analysis.

Flow-Assisted Cell Sorting for B cell populations

Single-cell suspension of splenocytes and lymph nodes was labeled with the antibodies listed in Table 1 and 7AAD in PBS supplemented with 2% FCS and 1% antibiotic–antimycotic (Gibco). Cells were sorted on a BD FACSAria II cytometer into the following groups: 1) 7AAD-TCR β -B220 + CD19^{int} and 2) 7AAD-TCR β -B220 + CD19^{lo}.

Adoptive Transfer of sorted B cell populations

Sorted cell populations were spun and resuspended in 1X PBS, and 2.2×10^5 cells were injected retro-orbitally into CD45 congenic WT B10.A animals. Cells were parked for

Table 1 Antibodies used for flow cytometric analysis

Antibody	Fluoro-chrome	Manufac-turer	Catalog #	Clone
7AAD		Biolegend	420,403	
CD4	APC-Cy7	BD Pharmin-gen	552,051	GK1.5
CD8b	FITC	Biolegend	140,404	53–5.8
TCRβ	APC	Biolegend	109,212	H57-597
CD25	PE	Biolegend	102,008	PC61
CD44	PE-Cy7	BD Pharmin-gen	560,569	IM7
CD11c	eFluor 450	eBioscience	48–0114-82	N418
CD11b	eFluor 450	eBioscience	48–0112-82	M1/70
B220	eFluor 450	Invitrogen	48–0452-82	RA3-682
NK1.1	eFluor 450	Invitrogen	48–5941-82	PK136
CD69	PE	Biolegend	104,508	H1.2F3
CD25	APC	Biolegend	102,012	PC61
TCRβ	PE-Cy7	Biolegend	109,222	H57-597
anti-Rat IgG	AF647	Ther-moFisher	A-21247	Polyclonal
CD19	APC-Cy7	BD Pharmin-gen	557,655	1D3
B220	PE	Biolegend	103,208	RA3-682
CD4	APC	Biolegend	100,412	GK1.5
CD8b	PE-Cy7	Biolegend	140,416	53–5.8
CD4	BV605	Biolegend	100,451	GK1.5
CD45.1	APC	Biolegend	110,714	A20
CD45.2	FITC	Biolegend	109,806	104
CD45.1	PE	Biolegend	110,708	A20
CD19	APC	Biolegend	152,410	1D3

60 days before harvesting lymph nodes and spleen from animals for flow cytometric analysis.

Acknowledgements We thank the University of Maryland Greenbaum Comprehensive Cancer Center Flow Cytometry Core and Dr. Xiaoxuan Fan for FACS Sorting and support. This work was supported by NIH Grants R01AI110719 and R21AI149076 (to N.J.S.).

Declarations

Conflict of interest The authors do not have any competing interests to disclose.

References

- June CH et al (2018) CAR T cell immunotherapy for human cancer. *Science* 359(6382):1361–1365
- Kalos M et al (2011) T cells with chimeric antigen receptors have potent antitumor effects and can establish memory in patients with advanced leukemia. *Sci Transl Med* 3(95):95ra73
- Kochenderfer JN, Rosenberg SA (2013) Treating B-cell cancer with T cells expressing anti-CD19 chimeric antigen receptors. *Nat Rev Clin Oncol* 10(5):267–276
- Kochenderfer JN et al (2010) Eradication of B-lineage cells and regression of lymphoma in a patient treated with autologous T cells genetically engineered to recognize CD19. *Blood* 116(20):4099–4102
- Martino M et al (2021) A Review of clinical outcomes of CAR T-Cell therapies for B-acute lymphoblastic leukemia. *Int J Mol Sci* 22(4):2150
- Penack O, Koenecke C (2020) Complications after CD19+ CAR T-Cell therapy. *Cancers (Basel)* 12(11):3445
- Xu X et al (2019) Mechanisms of relapse after CD19 CAR T-Cell therapy for acute lymphoblastic leukemia and Its prevention and treatment strategies. *Front Immunol* 10:2664
- Sotillo E et al (2015) Convergence of acquired mutations and alternative splicing of CD19 enables resistance to CART-19 immunotherapy. *Cancer Discov* 5(12):1282–1295
- Ledererova A et al (2021) Hypermethylation of CD19 promoter enables antigen-negative escape to CART-19 in vivo and in vitro. *J Immunother Cancer* 9(8):e002352
- Jacoby E et al (2016) CD19 CAR immune pressure induces B-precursor acute lymphoblastic leukaemia lineage switch exposing inherent leukaemic plasticity. *Nat Commun* 7:12320
- Kochenderfer JN et al (2010) Adoptive transfer of syngeneic T cells transduced with a chimeric antigen receptor that recognizes murine CD19 can eradicate lymphoma and normal B cells. *Blood* 116(19):3875–3886
- Pennell CA et al (2018) Human CD19-Targeted mouse T Cells induce B Cell aplasia and toxicity in human CD19 transgenic mice. *Mol Ther* 26(6):1423–1434
- Davila ML et al (2013) CD19 CAR-targeted T cells induce long-term remission and B Cell Aplasia in an immunocompetent mouse model of B cell acute lymphoblastic leukemia. *PLoS ONE* 8(4):e61338
- Hamieh M et al (2019) CAR T cell trogocytosis and cooperative killing regulate tumour antigen escape. *Nature* 568(7750):112–116
- Ruella M et al (2016) Dual CD19 and CD123 targeting prevents antigen-loss relapses after CD19-directed immunotherapies. *J Clin Invest* 126(10):3814–3826
- Gardner R et al (2016) Acquisition of a CD19-negative myeloid phenotype allows immune escape of MLL-rearranged B-ALL from CD19 CAR-T-cell therapy. *Blood* 127(20):2406–2410
- Cobaleda C et al (2007) Pax5: the guardian of B cell identity and function. *Nat Immunol* 8(5):463–470
- Shapiro-Shelef M, Calame K (2005) Regulation of plasma-cell development. *Nat Rev Immunol* 5(3):230–242
- Jones JD, Hamilton BJ, Rigby WF (2012) Rituximab mediates loss of CD19 on B cells in the absence of cell death. *Arthritis Rheum* 64(10):3111–3118

Publisher's Note Springer Nature remains neutral with regard to jurisdictional claims in published maps and institutional affiliations.